Against the Norm: Non Irving–Williams Transmetalation in Transition Metal Dimers

Against the Norm: Non Irving-Williams Transmetalation in Transition Metal Dimers

Sidney S. Woodhouse,[†] Tyson N. Dais,[†] Alvaro Etcheverry-Berríos,[‡] Euan K. Brechin,[‡] Joseph R. Lane,[¶] and Paul G. Plieger[*,†]

[†]*School of Natural Sciences, Massey University, Private Bag 11 222, Palmerston North, New Zealand*

[‡]*EaStCHEM School of Chemistry, The University of Edinburgh, David Brewster Road, Edinburgh, EH93FJ, Scotland, United Kingdom*

[¶]*Department of Chemistry, School of Science, University of Waikato, Private Bag 3105, Hamilton, New Zealand*

E-mail: p.g.plieger@massey.ac.nz

Abstract

We report the synthesis and characterisation of three dinuclear $3d3d$' complexes, $[Cu^{II}M^{II}\mathbf{L}(NO_3)_2]$ (M = Cu^{II} (**CuCu**) and Mn^{II} (**CuMn**)) and $[Mn^{II}{}_2\mathbf{L}(MeOH)_2(NO_3)_2]$ (**MnMn**) that utilise the ligand, $H_2\mathbf{L}$ (6,6'-Dimethoxy-2,2'-[(1,3-propylene)dioxybis(nitrilomethylidyne)]diphenol). The relative stabilities of these complexes were investigated using experimental and computational techniques, revealing a non-Irving-Williams transmetalation whereby a Mn^{II} ion can displace a Cu^{II} ion from its binding pocket in **CuCu** to yield the more stable **CuMn** complex. Magnetic characterisation of the reported complexes revealed an unexpected ferromagnetic coupling between the two Cu^{II} ions of **CuCu** with $J = +63.0$ cm^{-1}.

Introduction

The last few years have seen a continued interest in polynuclear complexes, specifically those consisting of first-row transition metal ions, for their use in fields such as catalysis,[1,2] magnetic materials,[3–5] separation,[6,7] and luminescence.[8] One fundamental property these fields share is stability and their need for stable complexes. Since the early 1950's, the relative stability of divalent first row transition metal complexes can be predicted using the Irving-Williams series. While the relative binding strengths of these +2 metal ions vary by ligand, they generally follow the trend of Mn < Fe < Zn < Co < Ni < Cu.[9] The trend can be loosely extended to include all first row transition metal based complexes, but is only definitive for mononuclear octahedral complexes, with numerous exceptions known for other geometries.[10,11]

A large proportion of complexes found in the literature have ligand frameworks derived from salen type Schiff bases as not only do they have simple preparations, they commonly have preformed multi-dentate coordination pockets, providing a driving force for coordination and formation of a stable complex.[12,13] One of the downfalls of Schiff base ligands however is the ease at which they undergo cleavage in acidic conditions. This is where *o*-alkyldiamines and bis-oximes have become popular as these structures, an extension to Schiff bases, are found to have greater stability towards acidic conditions.[14–18]

The stability of a complex can be both computationally determined and experimentally measured, but another approach is to investigate how the complex responds to a different environment or external stimuli. One method that can be used to investigate stability is transmetalation, the exchange of one or more metal ions without significantly altering the coordination environment. Transmetalation is most commonly seen throughout the literature in catalysis and cross-coupling reactions such as the Suzuki and Sonogashira reactions and as a straightforward method to produce new complexes with difficult syntheses.[19–21]

Our goal for this research was to investigate the relative stability of a series of transition metal complexes, specifically dinuclear homo- and heterometallic, and their asso-

ciated magnetic properties. Our complex framework stems from the ligand, $H_2\mathbf{L}$ (6,6'-Dimethoxy-2,2'-[(1,3-propylene)dioxybis(nitrilomethylidyne)]diphenol), which was chosen as it has two distinct coordination environments (Figure 1) and the literature has shown that its analogues are capable of producing polynuclear, and specifically dinuclear, complexes.[13,17,18] Our group has previously reported several exciting polynuclear structures with interesting magnetic and/or structural properties.[22–26] In this research we report the synthesis, transmetalation, X-ray structures, and computational and magnetic analyses on three dimeric complexes, $[Cu^{II}{}_2\mathbf{L}(NO_3)_2]$ (**CuCu**), $[Mn^{II}{}_2\mathbf{L}(MeOH)_2(NO_3)_2]$ (**MnMn**), and $[Cu^{II}Mn^{II}\mathbf{L}(NO_3)_2]$ (**CuMn**). The labelling of the complexes is directly related to the metal ions occupying the coordination pockets (M1M2, Figure 2). For example, **CuMn** has Cu^{II} in the inner pocket (M1) and Mn^{II} in the outer pocket (M2).

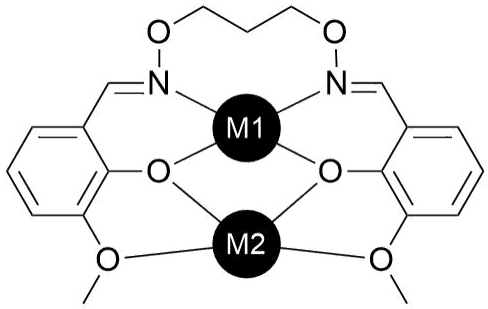

Figure 1: Schematic representation of the ligand, $H_2\mathbf{L}$, and its two distinct coordination pockets, M1 and M2.

Results and discussion

The ligand utilised for this series, $H_2\mathbf{L}$, was synthesised through three steps beginning with an adapted Gabriel synthesis where an acidic hydrolysis replaced the more typical Ing-Manske procedure, followed by a Schiff base condensation to give $H_2\mathbf{L}$ in 80% yield (Figure 2). For detailed procedures see the Supporting Information.

The solid state complexes **CuCu**, **MnMn**, and **CuMn** (CCDC deposition numbers 2184569 - 2184571) were synthesised from the methanolic reaction between ligand, $H_2\mathbf{L}$,

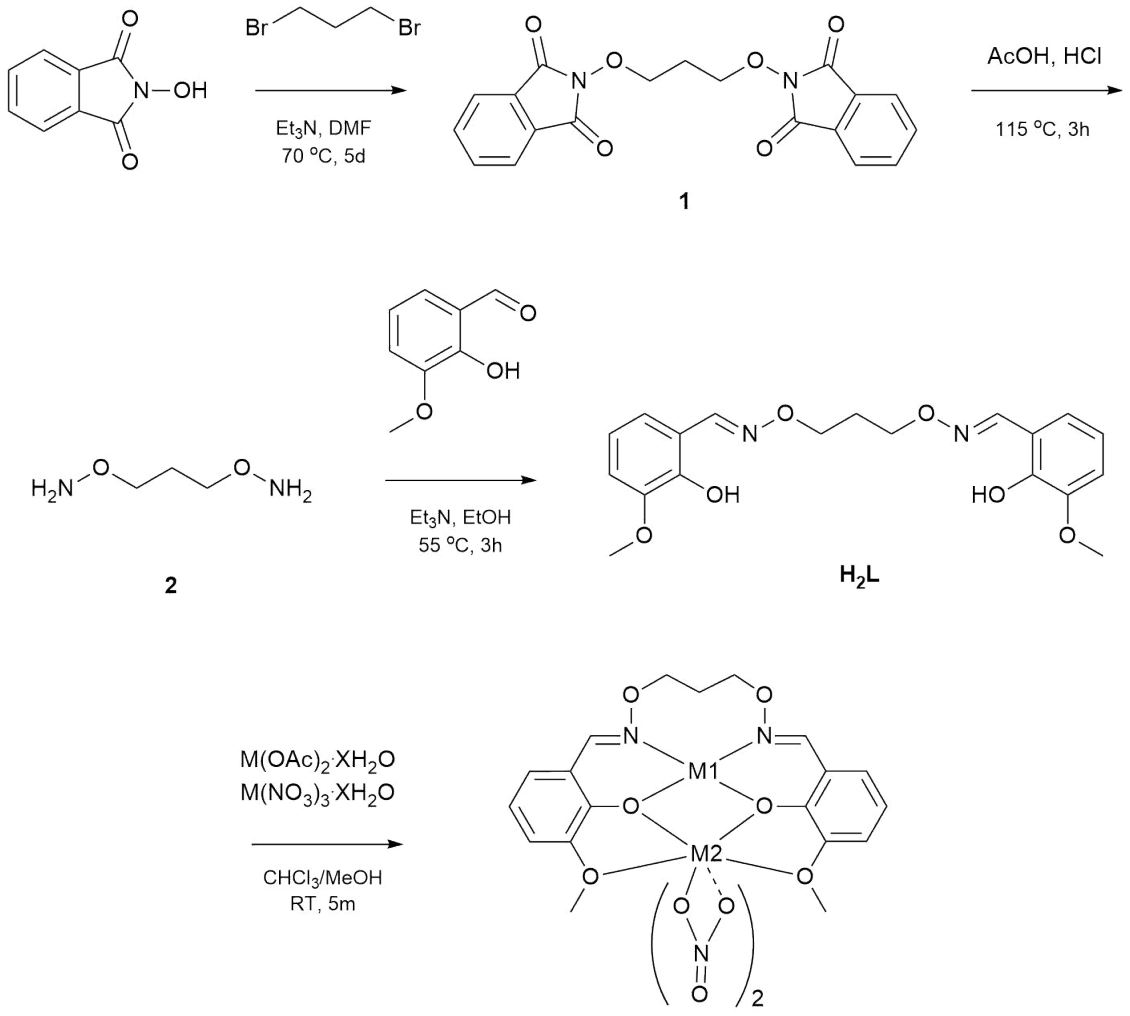

Figure 2: Synthethic route to producing 6,6'-dimethoxy-2,2-[(1,3-propylene)dioxybis(nitrilomethylidyne)]diphenol, H_2**L** and the dimeric complexes, **CuCu**, **MnMn**, and **CuMn**. See Supporting Information for detailed procedures.

$M(OAc)_2 \cdot xH_2O$, and $M(NO_3)_2 \cdot xH_2O$ (M = Cu and Mn) in a 1 : 1 : 1 molar ratio at room temperature (RT). For all complexes, a colour change from the pale yellow ligand solution to either a dark brown/green (**CuCu**), light brown (**MnMn**), or dark green (**CuMn**) solution confirmed successful coordination. The complexes were isolated by slow vapour diffusion of Et_2O into the reaction solution. X-ray quality crystals were obtained after a period of three (**CuCu** and **CuMn**) to four (**MnMn**) weeks.

Structural Analysis

The complexes were found to be either monoclinic (**CuCu** and **CuMn**), crystallising in the $P2_1/n$ space group or triclinic (**MnMn**), crystallising in the $P\bar{1}$ space group (Table S1). For all complexes, the general structure consists of a dinuclear complex where one unit of H_2**L** is coordinated to two metal ions. For **CuCu**, **MnMn**, and **CuMn**, the whole structure can be found within the asymmetric unit, with full structures shown in Figures 3-5.

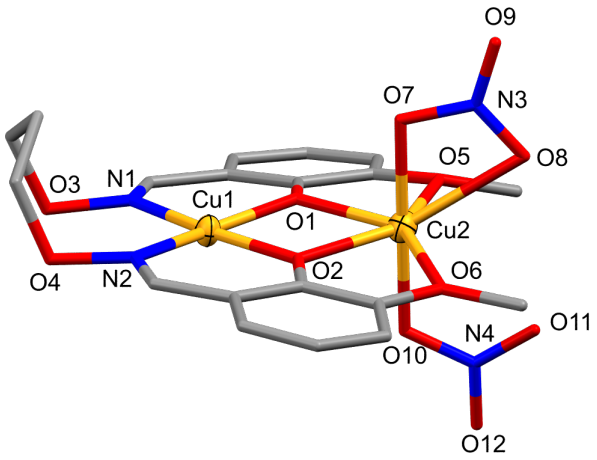

Figure 3: Full molecular structure of $[Cu^{II}_2\mathbf{L}(NO_3)_2]$, **CuCu**. Hydrogen atoms omitted for clarity and thermal ellipsoids shown at 70% probability level. Colour code: Cu^{II} = yellow, N = blue, O = red, and C = grey.

For complexes **CuCu** and **CuMn**, M1 (Cu1) is tetracoordinated with a square planar geometry and for **MnMn**, M1 (Mn1) is hexacoordinated with an octahedral geometry as de-

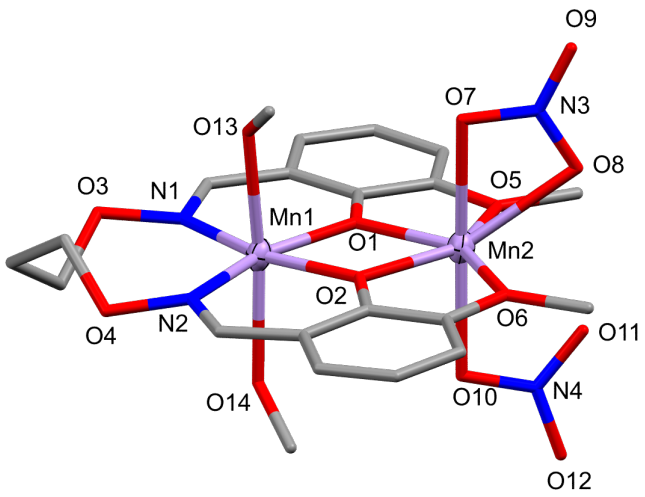

Figure 4: Full molecular structure of $[Mn^{II}_2\mathbf{L}(MeOH)_2(NO_3)_2]$, **MnMn**. Hydrogen atoms omitted for clarity and thermal ellipsoids shown at 70% probability level. Colour code: Mn^{II} = purple, N = blue, O = red, and C = grey.

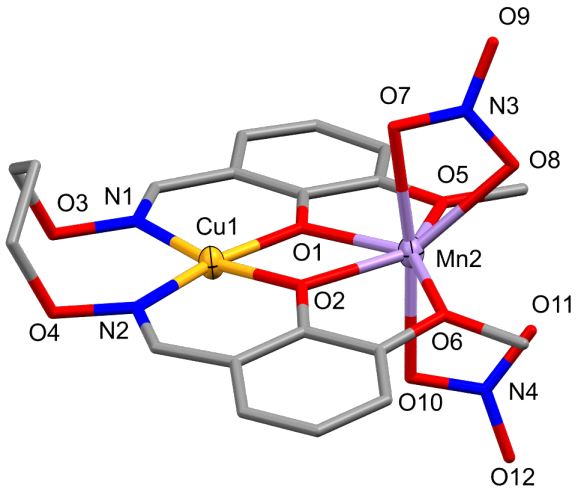

Figure 5: Full molecular structure of $[Cu^{II}Mn^{II}\mathbf{L}(NO_3)_2]$, **CuMn**. Hydrogen atoms omitted for clarity and thermal ellipsoids shown at 70% probability level. Colour code: Cu^{II} = yellow, Mn^{II} = purple, N = blue, O = red, and C = grey.

termined by SHAPE (Table S4).[27–31] For all complexes, M2 (Cu2 (**CuCu**) and Mn2 (**MnMn** and **CuMn**)) is heptacoordinated with a distorted capped trigonal prism geometry as determined by SHAPE (Table S4) with selected bond lengths and angles found in Tables S5 and S6.[27–29,32] For **CuCu** and **CuMn**, M1 has an N_2O_2 donor set consisting of two oximato nitrogens and two phenolato oxygens whereas for **MnMn**, M1 has an additional two axial oxygen donors, provided by MeOH molecules. M2 for all complexes has an O_7 donor set consisting of two phenolato oxygens, two methoxy oxygens, and two nitrate anions, one monodentate and the other bidentate. For both **MnMn** and **CuMn**, the second oxygen atom of the monodentate anion is weakly coordinated to M2 with bond lengths of 2.524(1) and 2.486(1) Å respectively (Mn-O_{NO_3} bond lengths are typically between 2.174 to 2.408 Å).[33–35] This difference can be seen visually (Figure 6) when comparing the M2-O10-N4 angle of the monodentate nitrate anion, as for **CuCu** the M2-O10-N4 angle is 117.4(2)° whereas for both **MnMn** and **CuMn** the angle is remarkably smaller at 100.9(2)° and 100.8(2)° respectively. These smaller angles bring the uncoordinated oxygen, O11, into the 'weakly coordinated' range. Moderate intermolecular hydrogen bonding is found in **MnMn** between the coordinated MeOH molecules (O13 and O14) and the nitrate anions (O7 and O12) above and below the molecular plane, as shown in Figure 7. When only considering one unit, the above-plane hydrogen bonding (2.771(3) Å) is between O13 (MeOH) and a coordinated oxygen, O7 (NO_3), whereas the below-plane hydrogen bonding (2.770(3) Å) occurs between O14 (MeOH) and a non-coordinated oxygen, O12 (NO_3). This difference can be attributed to the different M2-O10-N4 angles of the nitrate anions and the packing of the unit cell.

The most noticeable structural difference between the three complexes, is the structural arrangement of the oximato bridge. For complexes **CuCu** and **CuMn**, the nitrogen and oxygen atoms of the oximato bridge sit almost planar with the metal ions and aromatic rings, while the propylene bridge sits almost perpendicular (Figure 8). For **MnMn**, the octahedral coordination geometry of M1 causes the propylene bridge to zig-zag above and below the plane of the metal ions/aromatic rings. This has resulted in small differences in the angles

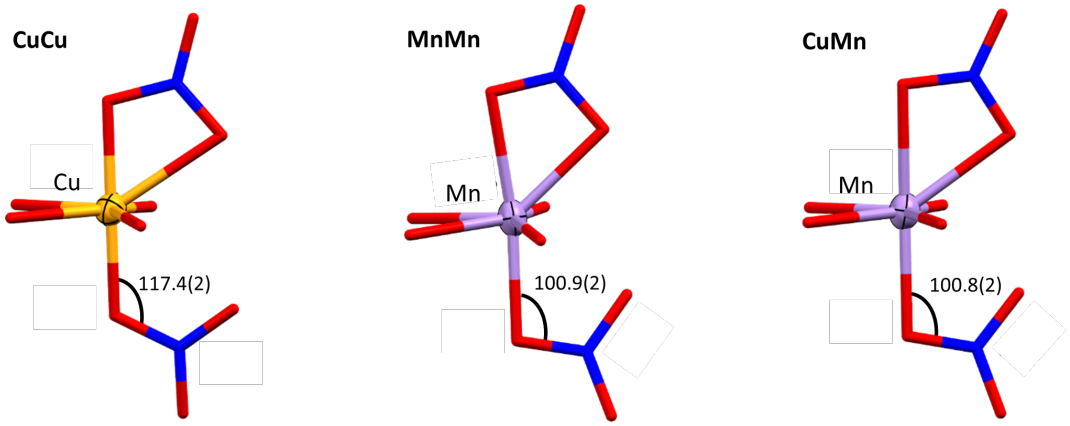

Figure 6: Schematic showing the differences in the nitrate anion coordination angle for complexes **CuCu**, **MnMn**, and **CuMn**. Hydrogen atoms omitted for clarity and thermal ellipsoids shown at 70% probability level. Colour code: Cu^{II} = yellow, Mn^{II} = purple, N = blue, and O = red.

surrounding the M1 ions between **CuCu**/**CuMn** and **MnMn**, with the greatest difference being the N1-M1-N2 angle, 102.04(1)° and 101.73(1)° for **CuCu** and **CuMn** respectively and 115.04(1)° for **MnMn** (Table S6). It is assumed that this structural difference in **MnMn** is the result of steric hinderance caused by the capping MeOH molecule.

The complexes, **CuCu**, **MnMn**, and **CuMn** have been characterised by ESI Mass spectrometry. The spectra indicate that the complexes do not completely remain intact when in solution as all complexes are present as $[M\text{-}NO_3]^+$ (m/z 559.98 (calculated: 559.98 for $C_{19}H_{20}N_3O_9Cu_2+H^+$), **CuCu**; 608.05 (calculated: 608.05 for $C_{21}H_{28}N_3O_{11}Mn_2+H^+$), **MnMn**; and 551.75 (calculated: 551.99 for $C_{19}H_{20}N_3O_9CuMn+H^+$), **CuMn**) instead of the more typical $[M+H]^+$.

ATR-IR spectroscopy has been performed on the three complexes with comparison to the free ligand, H_2**L** (Table S7). As the results from SCXRD have shown, the free ligand coordinates to the metal ions via the oximato N (C=N) and phenolato O atoms (C-O/Ar-O) therefore these stretches are expected to have shifted. The O-H (phenolato) stretch of the free ligand was observed at 3421 cm^{-1}, and disappeared for all three complexes indicating the coordination of the phenolato oxygen. A new O-H stretch was observed in **MnMn** at 3362 cm^{-1} corresponding to the coordinated MeOH molecules. The most characteristic

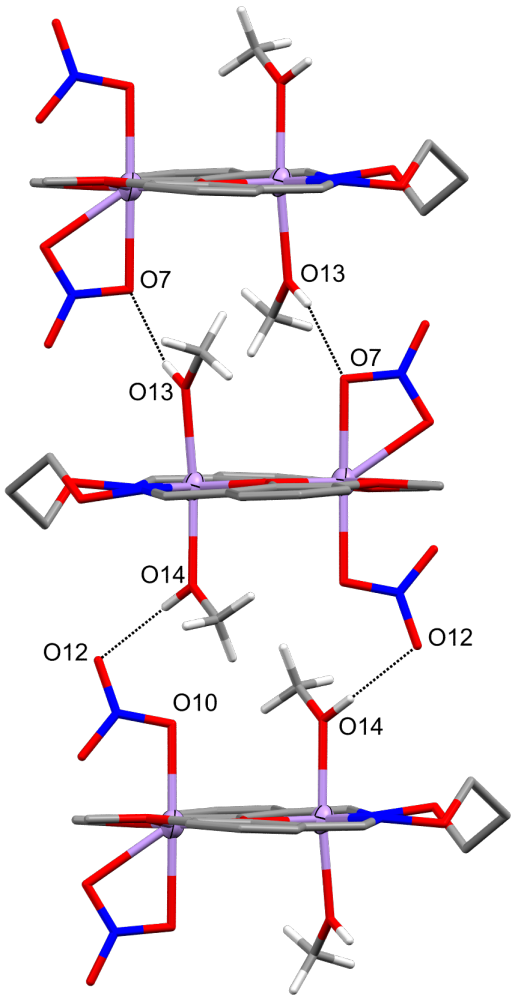

Figure 7: The hydrogen bonding network found in **MnMn**. Hydrogen atoms, apart from those of donor groups, have been omitted for clarity, hydrogen bonding represented as black dotted lines, and thermal ellipsoids shown at 70% probability level. Colour code: Mn^{II} = purple, N = blue, O = red, C = grey, and H = white.

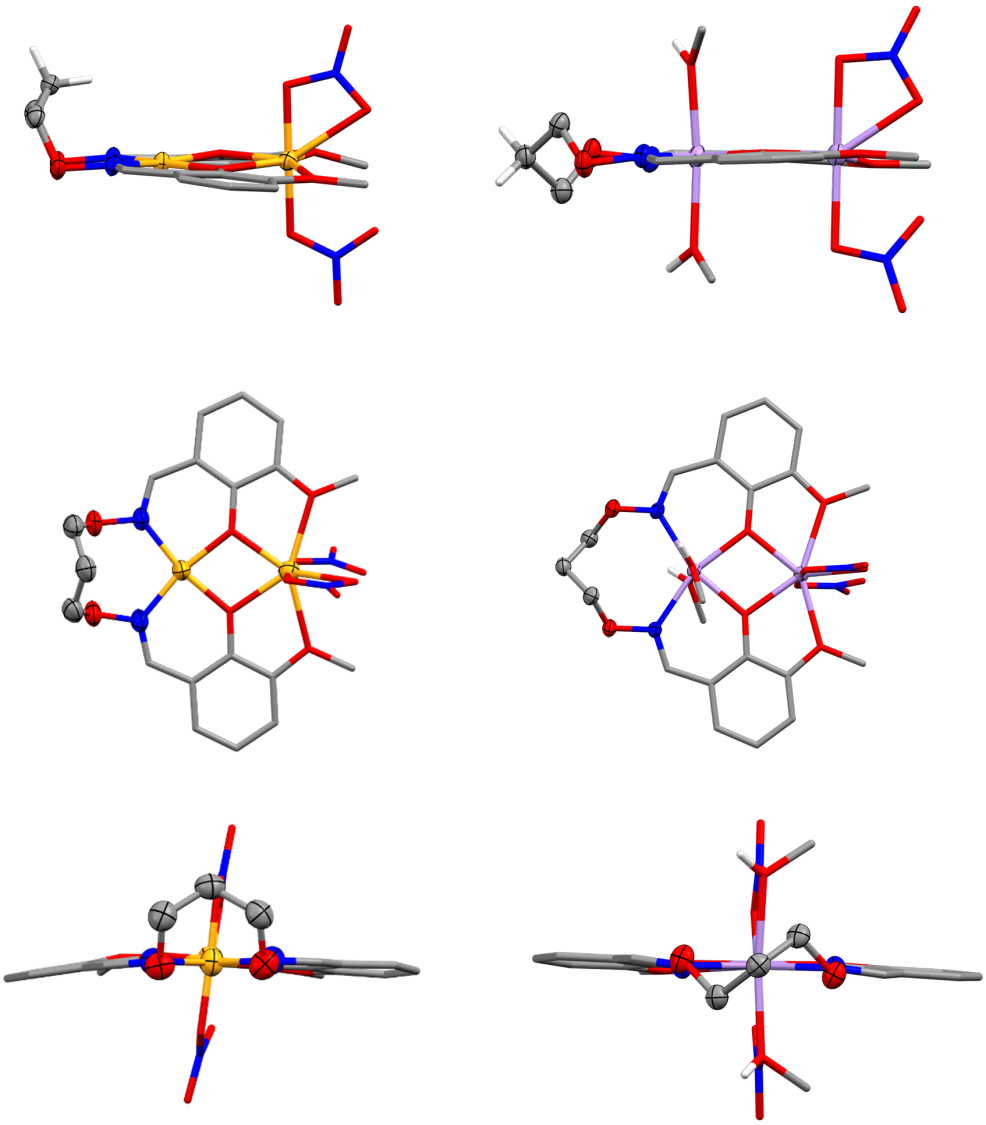

Figure 8: Schematic illustrating the structural differences between the oximato bridges for complexes **CuCu**/**CuMn** (left) and **MnMn** (right). Metal ions and the oximato bridges are shown as ellipsoids (70% probability) for ease of view and the hydrogen atoms of the central carbon are shown in the top view to illustrate the potential steric hinderance for **MnMn**. Non-interacting hydrogen atoms have been omitted for clarity. Colour code: Cu^{II} = yellow, Mn^{II} = purple, N = blue, O = red, C = grey, and H = white.

stretch for bis-oxime type ligands is the C=N stretch, which was observed at 1606 cm^{-1} for the free ligand and shifted slightly to 1605, 1604, and 1602 cm^{-1} for the complexes **CuCu**, **MnMn**, and **CuMn** respectively. The Ar-O stretch of the free ligand was seen at 1251 cm^{-1} and shifted to 1244 cm^{-1}, 1242 cm^{-1}, and 1244 cm^{-1} for **CuCu**, **MnMn**, and **CuMn** respectively. The coordinated nitrate stretches can be seen at approximately 1463, 1295, 1039, and 816 cm^{-1}. Previous research in the literature has found that the coordination of anions, which are capable of coordinating in various modes such as nitrate or acetate, can be determined by the difference between asymmetric and symmetric stretches.[36,37] For nitrate anions, bidentate coordination is found when the range between the stretches at approximately 1463 and 1298 cm^{-1} is between 175 - 181 cm^{-1}. As the three complexes have mixed coordination, the value was expected to be outside of this range, with differences of 161, 168, and 165 cm^{-1} respectively for **CuCu**, **MnMn**, and **CuMn**.

Transmetalation

Transmetalation reactions were performed to investigate the stability and metal ion preference of the coordination pockets to see the effect of the second metal ion and whether the Irving-Williams trend extends to both homo- and hetero-metallic dinuclear complexes and non-octahedral geometries.

Crystals of both **CuCu** and **MnMn** were dissolved in 0.025 mol/L methanolic solutions of $Mn(NO_3)_2 \cdot 4\,H_2O$ and $Cu(NO_3)_2 \cdot 3\,H_2O$ respectively and left to sit at RT for 24 hours, after which the solutions were filtered and set up for Et_2O vapour diffusion. After three weeks, dark green platelet shaped crystals were obtained from both reactions with SCXRD, AAS (Table S3 and Figure S2), and bond length analyses (Tables S5 and S6) revealing them to be **CuMn** (**CuMn1** and **CuMn2** respectively, CCDC deposition numbers 2209916 and 2209917). Transmetalation also occurred when 0.025 mol/L methanolic solutions of preformed **CuCu** and **MnMn** were mixed together at RT for 24 hours, after which the solution was set up for Et_2O vapour diffusion. Dark green platelet shaped crystals were

obtained after one week, and found to be **CuMn** by SCXRD. From these results we proposed that Cu^{II} was the most stable in the inner pocket and Mn^{II} the most stable in the outer pocket, suggesting that **CuMn** had the greatest overall stability.

As transmetalation reactions are often said to be irreversible processes, this was confirmed by attempting the transmetalation reactions on **CuMn**. Crystals of **CuMn** were soaked in 0.025 mol/L methanolic solutions of both $Mn(NO_3)_2 \cdot 4\,H_2O$ and $Cu(NO_3)_2 \cdot 3\,H_2O$, following the same method as mentioned above. The result for both reactions was the isolation of **CuMn** only, showing the transmetalation was indeed irreversible.

When considering these results from a structural view, they make sense as the smaller Cu^{II} ion was more stable in the smaller coordination pocket and the larger Mn^{II} ion was more stable in the larger coordination pocket. Additionally, the 4-coordinate geometry of the Cu^{II} ion retains the structural stability of the inner pocket, whereas the octahedral geometry of the Mn^{II} ion caused the N1-Mn-N2 angles to significantly increase (Table S6), decreasing the stability of the pocket. If we consider the findings using an Irving-Williams lens, although each individual coordination pocket has different donor groups (N_2O_2 versus O_4), both pockets (if considered individually) would be predicted to follow the Irving-Williams trend with the inclusion of Cu^{II} ions leading to the most stable complex.[9] Therefore, the overall prediction would be that the **CuCu** complex would be expected to be the most stable. Clearly, the larger coordination pocket and preference for seven-coordinate geometry favours Mn^{II} ions over Cu^{II} ions in the outer pocket.

Magnetic Analysis

In order to accurately model the three complexes computationally, an analysis of the spin states and magnetic exchange was required. The direct-current molar magnetic susceptibilities, χ, of the polycrystalline samples, **CuCu**, **MnMn**, and **CuMn** were measured in an applied magnetic field, $B = 0.1$ T, over $T = 2$ - 300 K temperature range. The experimental results are shown in Figure 9a as the $\chi_M T$ product versus T, where $\chi = M/B$ and M is the

magnetisation.

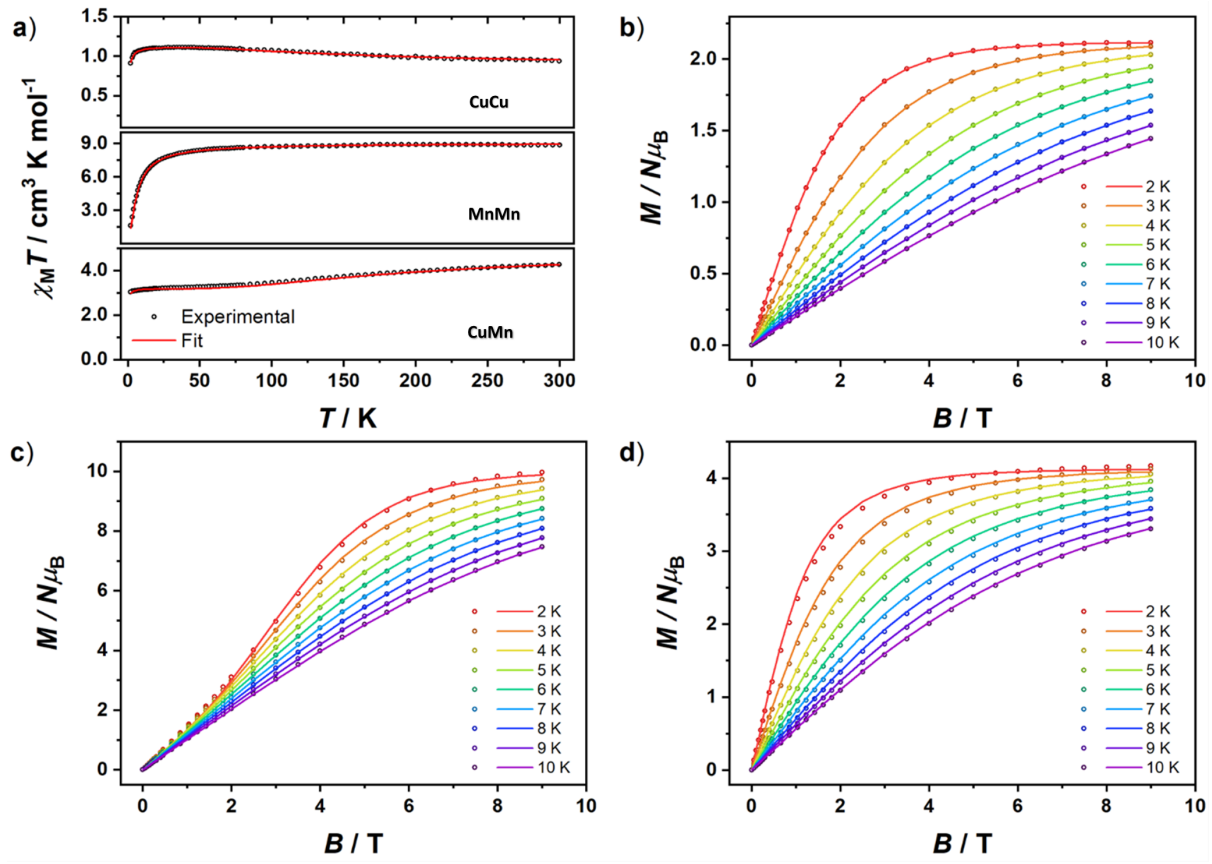

Figure 9: a) Plot of the $\chi_M T$ product versus T for **CuCu**, **MnMn**, and **CuMn** in an applied field, $B = 0.1$ T over the $T = 2$ - 300 K temperature range. Plot of magnetisation versus field data for **CuCu** (b), **MnMn** (c), and **CuMn** (d) in the $T = 2$ - 10 K and $B = 0.5$ - 9.0 T, temperature and field ranges, respectively. The solid lines represent the fit of the experimental data (circles) using spin-Hamiltonian (equation 1), as discussed in the text.

Upon cooling, the $\chi_M T$ value of **CuCu** slowly increases from 0.94 cm^3 K mol^{-1} at $T =$ 300 K to a maximum value of 1.11 cm^3 K mol^{-1} at $T = 36$ K, before decreasing to 0.90 cm^3 K mol^{-1} at 2 K. This behaviour is indicative of a ferromagnetic interaction between the two Cu^{II} ions, with the low T decrease assigned to antiferromagnetic intermolecular interactions, consistent with the packing of the molecules in the extended structure and the close contacts between the nitrate molecules on one complex and the Schiff base ligand on its neighbour (O(NO$_3$)$\cdots$(H)C, 3.159(4) Å, Figure S3). To better define the low temperature magnetic properties of **CuCu**, variable-temperature-variable-field (VTVB) magnetisation

measurements were performed in the temperature and field ranges T = 2 - 10 K and B = 0.5 - 9.0 T, respectively (Figure 9b). The VTVB magnetisation data of **CuCu** rises rapidly with increasing field, with the maximum value, 2.12 μ_{B}, at T = 2 K and B = 9.0 T. Both the susceptibility and magnetisation data are therefore consistent with the stabilisation of an S = 1 ground state. The susceptibility and magnetisation data were simultaneously fitted to an isotropic spin-Hamiltonian, equation 1, affording the best-fit parameters J = +63.0 cm^{-1} and g_{Cu} = 2.12. The fit requires inclusion of an intermolecular interaction term zJ = -0.10 cm^{-1}, consistent with the extended structure (Table 1). A search through the literature has revealed **CuCu** to have the largest ferromagnetic coupling for a Schiff base derived Cu^{II}_2 dimer to the best of our knowledge. The ferromagnetic exchange observed is unexpected based on previous magneto-structural correlations of O-bridged Cu^{II} dimers which consider only the Cu-O-Cu angles.[38–42] The Cu1-O-Cu2 angles in **CuCu** are 106.01(10)° and 105.22(10)° and would be expected to promote strong antiferromagnetic interactions based on this model as shown by similar Schiff based derived Cu^{II} dimers.[43–46] Thus, as discussed by Ruiz and coworkers,[47] other structural factors in **CuCu** including complex asymmetry, metal ion geometry, O-Cu-O-Cu torsion angles, the out-of-plane shift of the phenolato units, and the seven-coordinate Cu^{II} ion should be considered. This will require detailed theoretical calculations which are beyond the scope of this paper.

$$\hat{H} = -2\sum_{i<j} J_{ij}\hat{s}_i \cdot \hat{s}_j \tag{1}$$

For **MnMn**, the $\chi_{\mathrm{M}}T$ product at T = 300 K is 8.84 cm^3 K mol^{-1}, close to the value of 8.75 cm^3 K mol^{-1} expected for two uncorrelated S = 5/2 Mn^{II} ions with g = 2.00. Upon cooling, the $\chi_{\mathrm{M}}T$ product decreases slowly to a value of 8.71 cm^3 K mol^{-1} at 100 K and then more rapidly to 1.64 cm^3 K mol^{-1} at 2 K. This behaviour is indicative of a weak antiferromagnetic interaction between the two Mn^{II} ions. The VTVB magnetisation data of **MnMn** is consistent with this interpretation, initially increasing slowly at lower fields before saturating at a value of 9.95 μ_{B} at T = 2 K and B = 9.0 T, where the large, applied

field overcomes the weak exchange (Figure 9c). A simultaneous fit of the susceptibility and magnetisation data to equation 1 affords the best fit parameters J = -0.45 cm^{-1} and g_{Mn} = 2.03 (Table 1), in agreement with similar compounds in the literature.[48–50]

For **CuMn**, the $\chi_{\mathrm{M}}T$ product at T = 300 K is 4.25 cm^3 K mol^{-1}, somewhat lower than the value of 4.83 cm^3 K mol^{-1} expected for a $Cu^{II}Mn^{II}$ dimer assuming g_{Mn} = 2.00 and g_{Cu} = 2.20. Upon cooling, the $\chi_{\mathrm{M}}T$ product slowly decreases and then plateaus at a value of 3.24 cm^3 K mol^{-1} at T = 50 K. Below 50 K the $\chi_{\mathrm{M}}T$ value decreases once more reaching a value of 3.05 cm^3 K mol^{-1} at 2 K. This behaviour is indicative of a weak antiferromagnetic interaction between the two metal ions and an $S = 2$ ground state, with the low T (< 50 K) decrease in $\chi_{\mathrm{M}}T$ being attributed to intermolecular antiferromagnetic interactions, similar to those found in **CuCu**. This is corroborated by the VTVB data which saturates at a value of 4.18 μ_{B} at 2 K and B = 9.0 T. A simultaneous fit of the susceptibility and magnetisation data afforded the best-fit parameters J = -34.8 cm^{-1}, g_{av} = 2.06 and zJ = -0.01 cm^{-1} (Table 1), consistent with similar compounds reported in the literature.[51–53]

Table 1: Best-fit parameters for the complexes **CuCu**, **MnMn**, and **CuMn**

	CuCu	**MnMn**	**CuMn**
J (cm^{-1})	+63.0	-0.45	-34.8
g_M	2.12	2.03	2.06
zJ (cm^{-1})	-0.10	–	-0.01

Computational Analysis

A DFT study was also undertaken to determine the relative binding energies, based on the calculated Gibbs free energy, of the complexes to establish a trend in the energetic stability of the complexes. In-line with the experimental magnetic results, all computations on the **CuCu** complex were completed under a ferromagnetic regime (triplet state), while computations involving the **CuMn** and **MnMn** complexes were completed in a broken symmetry regime consistent with the presence of antiferromagnetically coupled high-spin Mn^{II}

(converged to the quintet and singlet state, respectively). To ensure consistency with synthetic methods, an implicit CPCM solvation model[54] was used to account for the influence of methanol throughout all calculations. Binding energies were calculated by finding the difference between the sum of Gibbs free energies of the products (complex and free water molecules) and the sum of Gibbs free energies of the starting materials (ligand, hydrated metal cations, nitrate anions, and methanol groups for **MnMn**). The resulting binding energies were found to give a trend of **CuMn** > **CuCu** > **MnMn**, **CuMn** (-127.1349 kcal mol^{-1}), **CuCu** (-125.7668 kcal mol^{-1}), and **MnMn** (-91.7206 kcal mol^{-1}), corroborating the experimentally observed transmetalation, and confirms that Cu^{II} ions are the most stable in the M1 pocket, further supported by the literature, which shows that Cu^{II} ions coordinate strongly in N_2O_2 pockets.[55–58] Upon geometry optimisation of the structures, the perpendicular (**CuCu** and **CuMn**) and zig-zag (**MnMn**) nature of the propylene bridge was retained. Broken symmetry DFT calculations based on the crystallographic geometries produced results in agreement with the experimental magnetic measurements (Table S2), further details including plots of magnetic orbitals can be found in Figures S4 - S10.

Conclusion

A series of three dinuclear homo- and heterometallic complexes, **CuCu**, **MnMn**, and **CuMn**, have been synthesised by a 1 : 1 : 1 reaction of ligand, $H_2\mathbf{L}$, $M(OAc)_2 \cdot xH_2O$, and $M(NO_3)_2 \cdot xH_2O$. All complexes have been characterised by SCXRD, transmetalation reactions, and magnetic and computational analyses. Through the use of transmetalation, it was found that the complex **CuMn** was the most stable. This result was somewhat unexpected as the canonical Irving-Williams monoatomic stability trend would suggest **CuCu** to be the most stable, however DFT based binding energy calculations revealed the **CuMn** complex to be more stable than **CuCu** by 1.37 kcal mol^{-1} or approximately 2.3 times thermal energy. Magnetic characterisation found both **MnMn** and **CuMn** to have antiferromagnetic

couplings and exchange parameters of J = -0.45 cm^{-1} and J = -34.8 cm^{-1} respectively. Unexpectedly, **CuCu** was found to have a ferromagnetic coupling between the Cu^{II} ions with an exchange parameter of J = +63.0 cm^{-1}, the largest ferromagnetic coupling for a Schiff base derived Cu^{II}_2 dimer reported in the literature. It's thought the unusual seven-coordinate geometry was a driving factor for the ferromagnetic coupling and lessened experimental stability. This has encouraged us to explore unusual coordination environments and their associated magnetic properties.

Acknowledgement

S.S.W. and P.G.P. thank Massey University for the award of Massey University Vice-Chancellors Doctoral scholarship to S.S.W. T.N.D. and P.G.P. thank Massey University for the award of Massey University Doctoral scholarship for Māori to T.N.D. E.K.B. thanks the European Union's Horizon 2020 research and innovation programme under the Marie Skłodowska-Curie grant agreement No. 882686 (MaSCHiP) for funding. The authors wish to acknowledge the use of New Zealand eScience Infrastructure (NeSI) high performance computing facilities as part of this research. New Zealand's national facilities are provided by NeSI and funded jointly by NeSI's collaborator institutions and through the Ministry of Business, Innovation & Employment's Research Infrastructure programme.

Supporting Information Available

Experimental procedures, structural and computational analyses, and characterisation data for the complexes, **CuCu**, **MnMn**, and **CuMn**.

References

(1) He, S.; Wang, F.; Tong, W. L.; Yiu, S. M.; Chan, M. C. W. Topologically diverse shape-persistent bis-(Zn–salphen) catalysts: efficient cyclic carbonate formation under mild conditions. *Chem. Commun.* **2016**, *52*, 1017–1020.

(2) Cozzi, P. G. Metal–Salen Schiff base complexes in catalysis: practical aspects. *Chem. Soc. Rev.* **2004**, *33*, 410–421.

(3) Liu, K.; Shi, W.; Cheng, P. Toward heterometallic single-molecule magnets: Synthetic strategy, structures and properties of 3d–4f discrete complexes. *Coord. Chem. Rev.* **2015**, *289-290*, 74–122.

(4) Mondal, K. C.; Sundt, A.; Lan, Y.; Kostakis, G. E.; Waldmann, O.; Ungur, L.; Chibotaru, L. F.; Anson, C. E.; Powell, A. K. Coexistence of Distinct Single-Ion and Exchange-Based Mechanisms for Blocking of Magnetization in a $Co^{II}_2Dy^{III}_2$ Single-Molecule Magnet. *Angew. Chem. Int. Ed.* **2012**, *51*, 7550–7554.

(5) Habib, F.; Brunet, G.; Vieru, V.; Korobkov, I.; Chibotaru, L. F.; Murugesu, M. Significant Enhancement of Energy Barriers in Dinuclear Dysprosium Single-Molecule Magnets Through Electron-Withdrawing Effects. *J. Am. Chem. Soc.* **2013**, *135*, 13242–13245.

(6) Forgan, R. S.; Davidson, J. E.; Fabbiani, F. P.; Galbraith, S. G.; Henderson, D. K.; Moggach, S. A.; Parsons, S.; Tasker, P. A.; White, F. J. Cation and anion selectivity of zwitterionic salicylaldoxime metal salt extractants. *Dalton Trans.* **2010**, *39*, 1763–1770.

(7) Coxall, R. A.; Lindloy, L. F.; Miller, H. A.; Parkin, A.; Parsons, S.; Tasker, P. A.; White, D. J. Solvent extraction of metal sulfates by zwitterionic forms of ditopic ligands. *Dalton Trans.* **2003**, *1*, 55–64.

(8) Liu, F.; Yang, F.; Chen, H.; Chen, Q.; Yan, P.; Li, G. Salen Type Homo-multinuclear Yb_3 and Yb_4 Complexes and Their NIR Luminescence. *J. Inorg. Organomet. Polym. Mater.* **2014**, *24*, 259–266.

(9) Irving, H.; Williams, R. J. P. The stability of transition-metal complexes. *J. Chem. Soc.* **1953**, 3192–3210.

(10) Cieslik, P.; Comba, P.; Dittmar, B.; Ndiaye, D.; Tóth, E.; Velmurugan, G.; Wadepohl, H. Exceptional Manganese(II) Stability and Manganese(II)/Zinc(II) Selectivity with Rigid Polydentate Ligands. *Angew. Chem. Int. Ed.* **2022**, *61*, e202115580.

(11) Solomon, L. R.; Bond, A. M.; Bixler, J. W.; Hallenbeck, D. R.; Logsdon, K. M. Stability of monofluoride complexes of the Irving-Williams series acceptors in methanol. *Inorg. Chem.* **1983**, *22*, 1644–1648.

(12) Costes, J. P.; Dahan, F.; Dupuis, A.; Laurent, J. P. A Genuine Example of a Discrete Bimetallic (Cu, Gd) Complex: Structural Determination and Magnetic Properties. *Inorg. Chem.* **1996**, *35*, 2400–2402.

(13) Dolai, M.; Mistri, T.; Panja, A.; Ali, M. Diversity in supramolecular self-assembly through hydrogen-bonding interactions of non-coordinated aliphatic –OH group in a series of heterodinuclear $Cu^{II}M$ (M = Na^{I}, Zn^{II}, Hg^{II}, Sm^{III}, Bi^{III}, Pb^{II} and Cd^{II}). *Inorg. Chim. Acta* **2013**, *399*, 95–104.

(14) Ren, Z.-L.; Gao, S.-X.; Zhang, Y.; Wang, L.; Dong, X.-Y. Synthesis and Characterization of Methoxy-Substituted Salamo-Type Bisoximes Based on Bis(aminooxy)alkane and 3-Methoxy-2-hydroxybenzaldehyde. *Asian J. Chem.* **2014**, *26*, 6940–6942.

(15) Enamullah, M.; Chamayou, A.-C.; Banu, K. S.; Kautz, A. C.; Janiak, C. Copper(II)-salicylaldehydate/-methoxy(pyridine-2-yl)methanolate complexes via in-situ hydrolysis of Schiff bases. *Inorg. Chim. Acta* **2017**, *464*, 186–194.

(16) Guo, S. Z.; Wang, J. F.; Feng, S. S.; Zhao, L. Co(II) and Ni(II) bis(salamo)-based tetraoxime complexes: Syntheses, structural characterizations, fluorescence properties, and Hirshfeld analyses. *J. Coord. Chem.* **2021**, 1–15.

(17) Bian, R.-N.; Wang, J.-F.; Xu, X.; Dong, X.-Y.; Ding, Y.-J. Investigation of mononuclear, dinuclear, and trinuclear transition metal (II) complexes derived from an asymmetric Salamo-based ligand possessing three different coordination modes. *Appl. Organomet. Chem.* **2021**, *35*, e6040.

(18) Zhang, Y.; Li, L. L.; Feng, S. S.; Feng, T.; Dong, W. K. Constructing Phenoxo-Bridged Heterobimetallic [$Zn(II)_2M(II)$] (M = Sr and Ba) Salamo-Based Complexes. *Russ. J. Gen. Chem.* **2021**, *91*, 2069–2078.

(19) Kumar, R.; Kaur, R.; Rana, S.; Kataria, R.; Sahoo, S. C. Single-crystal-to-single-crystal mediated metal exchange from Zn(II) to Cu(II) and diverse structures in Zn/Cu coordination polymers using pyridylmethionine ligand. *J. Mol. Struct.* **2021**, *1227*, 129527–129533.

(20) Martín, J.; Gómez-Bengoa, E.; Genoux, A.; Nevado, C. Synthesis of Cyclometalated Gold(III) Complexes via Catalytic Rhodium to Gold(III) Transmetalation. *Angew. Chem. Int. Ed.* **2022**, *61*, e202116755.

(21) Krupiński, P.; Terlecki, M.; Kornowicz, A.; Justyniak, I.; Prochowicz, D.; van Leusen, J.; Kögerler, P.; Lewiński, J. Tetrahedral $M_4(\mu_4{-}O)$ Motifs Beyond Zn: Efficient One-Pot Synthesis of Oxido–Amidate Clusters via a Transmetalation/Hydrolysis Approach. *Inorg. Chem.* **2022**, *61*, 7869–7877.

(22) Woodhouse, S. S.; De Silva, D. N. T.; Jameson, G. B.; Cutler, D. J.; Sanz, S.; Brechin, E. K.; Davies, C. G.; Jameson, G. N. L.; Plieger, P. G. New salicylaldoximato-borate ligands resulting from anion hydrolysis and their respective copper and iron complexes. *Dalton Trans.* **2019**, *48*, 11872–11881.

(23) Woodhouse, S. S.; Dais, T. N.; Payne, E. H.; Singh, M. K.; Brechin, E. K.; Plieger, P. G. The structural manipulation of a series of Ni_4 defective dicubanes: Synthesis, X-ray Structures, Magnetic and Computational analyses. *Dalton Trans.* **2021**, *50*, 5318–5326.

(24) Dais, T. N.; Takano, R.; Yamaguchi, Y.; Ishida, T.; Plieger, P. G. Metallocyclic Cu^{II}–Ln^{III} Single-Molecule Magnets from the Self-Assembly of 1,4-Diformylnaphthalene-2,3-diol. *ACS Omega* **2022**, *7*, 5537–5546.

(25) Dais, T. N.; Takano, R.; Ishida, T.; Plieger, P. G. Lanthanide induced variability in localised Co^{II} geometries of four triangular $L_3Co_3{}^{II}Ln^{III}$ complexes. *RSC Adv.* **2022**, *12*, 4828–4835.

(26) Dais, T. N.; Takano, R.; Ishida, T.; Plieger, P. G. Self-assembly of non-macrocyclic triangular Ni_3Ln clusters. *Dalton Trans.* **2022**, *51*, 1446–1453.

(27) Pinsky, M.; Avnir, D. Continuous Symmetry Measures. 5. The Classical Polyhedra. *Inorg. Chem.* **1998**, *37*, 5575–5582.

(28) Casanova, D.; Cirera, J.; Llunell, M.; Alemany, P.; Avnir, D.; Alvarez, S. Minimal Distortion Pathways in Polyhedral Rearrangements. *J. Am. Chem. Soc.* **2004**, *126*, 1755–1763.

(29) Cirera, J.; Ruiz, E.; Alvarez, S. Shape and Spin State in Four-Coordinate Transition-Metal Complexes: The Case of the d_6 Configuration. *Chem. Eur. J.* **2006**, *12*, 3162–3167.

(30) Cirera, J.; Alemany, P.; Alvarez, S. Mapping the Stereochemistry and Symmetry of Tetracoordinate Transition-Metal Complexes. *Chem. Eur. J.* **2004**, *10*, 190–207.

(31) Alvarez, S.; Avnir, D.; Llunell, M.; Pinsky, M. Continuous symmetry maps and shape classification. The case of six-coordinated metal compounds. *New J. Chem.* **2002**, *26*, 996–1009.

(32) Casanova, D.; Alemany, P.; Bofill, J. M.; Alvarez, S. Shape and Symmetry of Heptacoordinate Transition-Metal Complexes: Structural Trends. *Chem. Eur. J.* **2003**, *9*, 1281–1295.

(33) Branzea, D. G.; Madalan, A. M.; Ciattini, S.; Avarvari, N.; Caneschi, A.; Andruh, M. New heterometallic coordination polymers constructed from 3d–3d binuclear nodes. *New J. Chem.* **2010**, *34*, 2479–2490.

(34) Costes, J.-P.; Garcia-Tojal, J.; Tuchagues, J.-P.; Vendier, L. Structural and Magnetic Study of a Trinuclear Mn^{II}–Gd^{III}–Mn^{II} Complex. *Eur. J. Inorg. Chem.* **2009**, *2009*, 3801–3806.

(35) McLellan, R.; Palacios, M. A.; Sanz, S.; Brechin, E. K.; Dalgarno, S. J. Importance of Steric Influences in the Construction of Multicomponent Hybrid Polymetallic Clusters. *Inorg. Chem.* **2017**, *56*, 10044–10053.

(36) Pu, L.-M.; An, X.-X.; Liu, C.; Long, H.-T.; Zhao, L. Insights into crystal structures, supramolecular architectures and antioxidant activities of self-assembled fluorescent hetero-multinuclear [Cu(II)-Ln(III)] (Ln = La, Ce, Pr and Nd) salamo-like complexes. *Appl. Organomet. Chem.* **2020**, *34*, e5980.

(37) Dong, Y.-J.; Ma, J.-C.; Zhu, L.-C.; Dong, W.-K.; Zhang, Y. Four 3d–4f heteromultinuclear zinc(II)–lanthanide(III) complexes constructed from a distinct hexadentate N_2O_2-type ligand: syntheses, structures and luminescence properties. *J. Coord. Chem.* **2017**, *70*, 103–115.

(38) Crawford, V. H.; Richardson, H. W.; Wasson, J. R.; Hodgson, D. J.; Hatfield, W. E. Relationship Between the Singlet-Triplet Splitting and the Cu-O-Cu Bridge Angle in Hydroxo-Bridged Copper Dimers. *Inorg. Chem.* **1976**, *15*, 2107–2110.

(39) Thompson, L. K.; Mandal, S. K.; Tandon, S. S.; Bridson, J. N.; Park, M. K. Magnetostructural Correlations in Bis(μ_2-phenoxide)-Bridged Macrocyclic Dinuclear Cop-

per(II) Complexes. Influence of Electron-Withdrawing Substituents on Exchange Coupling. *Inorg. Chem.* **1996**, *35*, 3117–3125.

(40) Black, D.; Blake, A. J.; Dancey, K. P.; Harrison, A.; McPartlin, M.; Parsons, S.; Tasker, P. A.; Whittaker, G.; Schröder, M. Synthesis, structures and magnetochemistry of binuclear cobalt(II), nickel(II) and copper(II) complexes of 2,6-diformyl-4-methylphenol dioxime. *J. Chem. Soc., Dalton Trans.* **1998**, 3953–3960.

(41) Venegas-Yazigi, D.; Aravena, D.; Spodine, E.; Ruiz, E.; Alvarez, S. Structural and electronic effects on the exchange interactions in dinuclear bis(phenoxo)-bridged copper(II) complexes. *Coord. Chem. Rev.* **2010**, *254*, 2086–2095.

(42) Mondal, D.; Majee, M. C.; Bhattacharya, K.; Long, J.; Larionova, J.; Khusniyarov, M. M.; Chaudhury, M. Crossover from Antiferromagnetic to Ferromagnetic Exchange Coupling in a New Family of Bis-(μ-phenoxido)dicopper(II) Complexes: A Comprehensive Magneto–Structural Correlation by Experimental and Theoretical Study. *ACS Omega* **2019**, *4*, 10558–10570.

(43) Costes, J.-P.; Duhayon, C.; Vendier, L.; Mota, A. J. Reactions of a series of ZnL, CuL and NiL Schiff base and non-Schiff base complexes with MCl_2 salts (M = Cu, Ni, Mn): syntheses, structures, magnetic properties and DFT calculations. *New J. Chem.* **2018**, *42*, 3683–3691.

(44) O'Connor, C. J.; Freyberg, D. P.; Sinn, E. Relation between structure and magnetic exchange interactions in bis(hexafluoroacetylacetonato)N,N'-ethylenebis[2-hydroxypropiophenoneiminato-N,O(2-)]copper(II)M'(II), Cu((prp)$_2$en)M, where M' = Cu, Ni, and Mn. Crystal structures of the complexes (M((prp)$_2$en)M, where M = Cu and Ni and M' = Cu, Co, and Mn. *Inorg. Chem.* **1979**, *18*, 1077–1088.

(45) Lucas, C. R.; Byrne, J. M. D.; Collins, J. L.; Dawe, L. N.; Miller, D. O. Copper(II)

complexes of open-chain thioether ligands terminated by salicylaldimine functionality. *Can. J. Chem.* **2011**, *89*, 1190–1201.

(46) Maity, D.; Drew, M. G. B.; Godsell, J. F.; Roy, S.; Mukhopadhyay, G. Synthesis and characterization of Cu(II) complexes of tetradentate and tridentate symmetrical Schiff base ligands involving *o*-phenelenediamine, salicylaldehyde and diacetylmonoxime. *Transition Met. Chem.* **2010**, *35*, 197–204.

(47) Ruiz, E.; Alemany, P.; Alvarez, S.; Cano, J. Structural Modelling and Magneto-Structural Correlations for Hydroxo-Bridged Copper(II) Binuclear Complexes. *Inorg. Chem.* **1997**, *36*, 3683–3688.

(48) Golombek, A. P.; Hendrich, M. P. Quantitative analysis of dinuclear manganese(II) EPR spectra. *J. Magn. Reson.* **2003**, *165*, 33–48.

(49) Gultneh, Y.; Tesema, Y. T.; Yisgedu, T. B.; Butcher, R. J.; Wang, G.; Yee, G. T. Studies of a Dinuclear Manganese Complex with Phenoxo and Bis-acetato Bridging in the Mn_2(II, II) and Mn_2(II, III) States: Coordination Structural Shifts and Oxidation State Control in Bridged Dinuclear Complexes. *Inorg. Chem.* **2006**, *45*, 3023–3033.

(50) Arora, H.; Barman, S. K.; Lloret, F.; Mukherjee, R. Isostructural Dinuclear Phenoxo-/Acetato-Bridged Manganese(II), Cobalt(II), and Zinc(II) Complexes with Labile Sites: Kinetics of Transesterification of 2-Hydroxypropyl-p-nitrophenylphosphate. *Inorg. Chem.* **2012**, *51*, 5539–5553.

(51) Dutta, S.; Mayans, J.; Ghosh, A. Facile synthesis of a new Cu(II) complex with an unsymmetrical ligand and its use as an O_3 donor metalloligand in the synthesis of Cu(II)–Mn(II) complexes: structures, magnetic properties, and catalytic oxidase activities. *Dalton Trans.* **2020**, *49*, 1276–1291.

(52) Luo, S.; Sun, X.; Zeng, B.; Zheng, P. From antiferromagnetic to ferromagnetic exchange

in a family of phenoxido-bridged heterodinuclear Cu(II)-Mn(II) complexes: A magneto-structural theoretical study. *Polyhedron* **2021**, *194*, 114955–114962.

(53) Birkelbach, F.; Winter, M.; Floerke, U.; Haupt, H.-J.; Butzlaff, C.; Lengen, M.; Bill, E.; Trautwein, A. X.; Wieghardt, K.; Chaudhuri, P. Exchange Coupling in Homo- and Heterodinuclear Complexes $Cu^{II}M$ [M = Cr(III), Mn(III), Mn(II), Fe(III), Co(III), Co(II), Ni(II), Cu(II), Zn(II)]. Synthesis, Structures, and Spectroscopic Properties. *Inorg. Chem.* **1994**, *33*, 3990–4001.

(54) Barone, V.; Cossi, M. Quantum Calculation of Molecular Energies and Energy Gradients in Solution by a Conductor Solvent Model. *J. Phys. Chem. A* **1998**, *102*, 1995–2001.

(55) Coxall, R. A.; Lindloy, L. F.; Miller, H. A.; Parkin, A.; Parsons, S.; Tasker, P. A.; White, D. J. Solvent extraction of metal sulfates by zwitterionic forms of ditopic ligands. *Dalton Trans.* **2003**, *1*, 55–64.

(56) Wenzel, M.; Bruere, S. R.; Knapp, Q. W.; Tasker, P. A.; Plieger, P. G. Zwitterionic dicopper helicates: anion encapsulation and binding studies. *Dalton Trans.* **2010**, *39*, 2936–2941.

(57) Stevens, J. R.; Plieger, P. G. Anion-driven conformation control and enhanced sulfate binding utilising aryl linked salicylaldoxime dicopper helicates. *Dalton Trans.* **2011**, *40*, 12235–12241.

(58) Wenzel, M.; Knapp, Q. W.; Plieger, P. G. A bis-salicylaldoximato-copper(II) receptor for selective sulfate uptake. *Chem. Commun.* **2011**, *47*, 499–501.

TOC Graphic

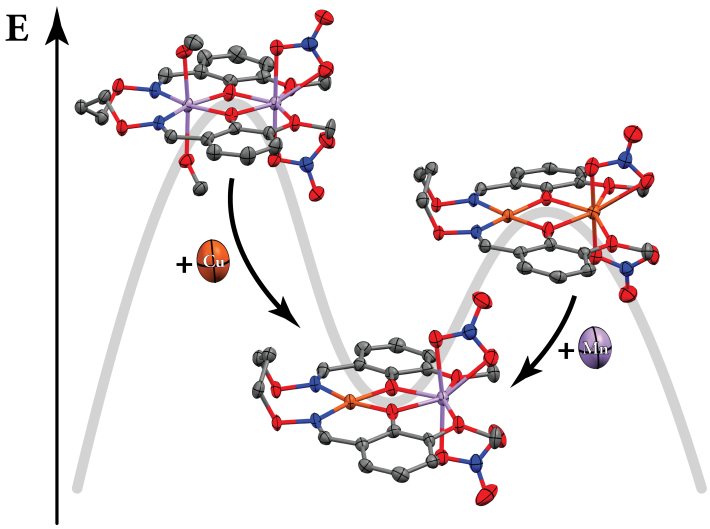

An investigation into the complex stability of a series of Cu and Mn dimers using transmetalation and computational analyses and their associated magnetic properties.

TOC Graphic

An investigation into the complex stability of a series of Cu and Mn dimers using transmetalation and computational analyses and their associated magnetic properties.